

J= P production vs Transverse Momentum and Rapidity
in p+ p Collisions at $\sqrt{s} = 200$ GeV

- A . A dare,⁸ S . A fanasiev,²² C . A idala,⁹ N N . A jitinand,⁴⁸ Y . Akiba,^{42,43} H . Al-Bataineh,³⁷ J . Alexander,⁴⁸
 K . A oki,^{27,42} L . A phoëtche,⁵⁰ R . A mendariz,³⁷ S H . A ronson,³ J . A sai,⁴³ E T . A tom ssa,²⁸ R . A verbeck,⁴⁹
 T C . Awes,³⁸ B . A zmoun,³ V . Babintsev,¹⁸ G . Baksay,¹⁴ L . Baksay,¹⁴ A . Baldissari,¹¹ K N . Barish,⁴ P D . Barnes,³⁰
 B . Bassalleck,³⁶ S . Bathe,⁴ S . Batsouli,³⁸ V . Baublis,⁴¹ A . Bazilevsky,³ S . Belikov,³ R . Bennett,⁴⁹ Y . Berdnikov,⁴⁵
 A A . Bickley,⁸ J G . Boissevain,³⁰ H . Borel,¹¹ K . Boyle,⁴⁹ M L . Brooks,³⁰ H . Buesching,³ V . Bumazhnov,¹⁸
 G . Bunce,^{3,43} S . Butsyk,^{30,49} S . Campbell,⁴⁹ B S . Chang,⁵⁷ J .L . Charvet,¹¹ S . Chemichenko,¹⁸ J . Chiba,²³
 C Y . Chi,⁹ M . Chiu,¹⁹ I J . Choi,⁵⁷ T . Chujo,⁵⁴ P . Chung,⁴⁸ A . Churyn,¹⁸ V . Cianciolo,³⁸ C R . Cleven,¹⁶
 B A . Cole,⁹ M P . Comets,³⁹ P . Constantin,³⁰ M . C sanad,¹³ T . Csorgo,²⁴ T . Dahms,⁴⁹ K . Das,¹⁵ G . David,³
 M B . Deaton,¹ K . D ehmelt,¹⁴ H . D elagrange,⁵⁰ A . Denisov,¹⁸ D . d'Enterria,⁹ A . D eshpande,^{43,49} E . J . Desmond,³
 O . Dietzsch,⁴⁶ A . D ion,⁴⁹ M . D onadelli,⁴⁶ O . D rapier,²⁸ A . D rees,⁴⁹ A K . D ubey,⁵⁶ A . D urum,¹⁸ V . D zhordzhadze,⁴
 Y . V . E frenko,³⁸ J . Egdem ir,⁴⁹ F . Ellinghaus,⁸ W . S . Em am,⁴ A . Enokizono,²⁹ H . En'yo,^{42,43} S . E sum i,⁵³
 K O . Eysen,⁴ D E . Fields,^{36,43} M . Finger,^{5,22} M . Finger, Jr.,^{5,22} F . Fleuret,²⁸ S L . Fokin,²⁶ Z . Fraenkel,⁵⁶
 J E . Frantz,⁴⁹ A . Franz,³ A D . Frawley,¹⁵ K . Fujiwara,⁴² Y . Fukao,^{27,42} T . Fusayasu,³⁵ S . G adrat,³¹ I . Garishvili,⁵¹
 A . G lenn,⁸ H . Gong,⁴⁹ M . Gonin,²⁸ J . G osset,¹¹ Y . G oto,^{42,43} R . G ranier de Cassagnac,²⁸ N . G rau,²¹
 S .V . G reene,⁵⁴ M . G rosse Perdekamp,^{19,43} T . G unji,⁷ H .A . G ustafsson,³² T . H achiya,¹⁷ A . H adj H enni,⁵⁰
 C . Haegemann,³⁶ J S . H aggerty,³ H . Hamagaki,⁷ R . Han,⁴⁰ H . Harada,¹⁷ E P . Hartouni,²⁹ K . Hanuna,¹⁷
 E . Haslum,³² R . Hayano,⁷ M . He ner,²⁹ T K . Hemmick,⁴⁹ T . H ester,⁴ X . He,¹⁶ H . H iejima,¹⁹ J C . Hill,²¹
 R . Hobbs,³⁶ M . H ohlmann,¹⁴ W . Holzmann,⁴⁸ K . Homma,¹⁷ B . Hong,²⁵ T . Horaguchi,^{42,52} D . Homback,⁵¹
 T . Ichihara,^{42,43} K . Imai,^{27,42} M . Inaba,⁵³ Y . Inoue,^{44,42} D . Isenhower,¹ L . Isenhower,¹ M . Ishihara,⁴² T . Isobe,⁷
 M . Issah,⁴⁸ A . Isupov,²² B V . Jacak,⁴⁹ J . Jia,⁹ J . Jin,⁹ O . Jinnouchi,⁴³ B M . Johnson,³ K S . Joo,³⁴ D . Jouan,³⁹
 F . K aihara,⁷ S . Kametani,^{7,55} N . Kamihara,⁴² J . Kam in,⁴⁹ M . Kaneta,⁴³ J H . Kang,⁵⁷ H . Kanou,^{42,52} D . Kawall,⁴³
 A .V . K astantsev,²⁶ A . Khanzadeev,⁴¹ J .K ikuchi,⁵⁵ D H . K im,³⁴ D J .K im,⁵⁷ E .K im,⁴⁷ E .K inney,⁸ A .K iss,¹³
 E .K istenev,³ A .K iyomichi,⁴² J .K lay,²⁹ C .K lein-Boesing,³³ L .K ochenda,⁴¹ V .K ochetkov,¹⁸ B .K omkov,⁴¹
 M .K onno,⁵³ D .K otchetkov,⁴ A .K ozlov,⁵⁶ A .K ral,¹⁰ A .K ravitz,⁹ J .K ubart,^{5,20} G .J .K unde,³⁰ N .K urihara,⁷
 K .K urita,^{44,42} M .J .K weon,²⁵ Y .K won,^{51,57} G .S .K yle,³⁷ R .L acey,⁴⁸ Y .S .L ai,⁹ J .G .L apie,²¹ A .Lebedev,²¹
 D M .Lee,³⁰ M K .Lee,⁵⁷ T .Lee,⁴⁷ M .J .Leitch,³⁰ M A L .Leite,⁴⁶ B .Lenzi,⁴⁶ T .Liska,¹⁰ A .Litvinenko,²²
 M X .Liu,³⁰ X .Li,⁶ B .Love,⁵⁴ D .Lynch,³ C F .M aguire,⁵⁴ Y .I .M akdisi,³ A .M alakhov,²² M D .M alik,³⁶
 V .I .M anko,²⁶ Y .M ao,^{40,42} L .M asek,^{5,20} H .M asui,⁵³ F .M atathias,⁹ M .M cC umber,⁴⁹ P .L .M cG aughey,³⁰
 Y .M iake,⁵³ P .M ikes,^{5,20} K .M iki,⁵³ T E .M iller,⁵⁴ A .M ilov,⁴⁹ S .M ioduszewski,³ M .M ishra,² J T .M itchell,³
 M .M itrovski,⁴⁸ A .M orreale,⁴ D .P .M orrison,³ T .V .M oukhanova,²⁶ D .M ukhopadhyay,⁵⁴ J .M urata,^{44,42}
 S .N agamiya,²³ Y .N agata,⁵³ J L .N agle,⁸ M .N aglis,⁵⁶ I .N akagawa,^{42,43} Y .N akam iya,¹⁷ T .N akamura,¹⁷
 K .N akano,^{42,52} J .N ewby,²⁹ M .N guyen,⁴⁹ B E .N orman,³⁰ A S .N yanin,²⁶ E .O B rien,³ S X .O da,⁷ C A .O gilvie,²¹
 H .O hnishi,⁴² H .O kada,^{27,42} K .O kada,⁴³ M .O ka,⁵³ O .O .O m i Wade,¹ A .O skarsson,³² M .O uchida,¹⁷
 K .O zawa,⁷ R .P ak,³ D .P al,⁵⁴ A P .T .P albunek,³⁰ V .P antuev,⁴⁹ V .P papavassiliou,³⁷ J .Park,⁴⁷ W .J .Park,²⁵
 S F .P ate,³⁷ H .P ei,²¹ J .C .P eng,¹⁹ H .P ereira,¹¹ V .P eresedov,²² D .Y u .P eressounko,²⁶ C .P inkenburg,³
 M L .P urschke,³ A K .P urwar,³⁰ H .Q u,¹⁶ J .R ak,³⁶ A .R akotoza ndrabe,²⁸ I .R avinovich,⁵⁶ K F .R ead,^{38,51}
 S .R embeczki,¹⁴ M .R euter,⁴⁹ K .R eygers,³³ V .R iabov,⁴¹ Y .R iabov,⁴¹ G .R oche,³¹ A .R om ana,²⁸, M .R osati,²¹
 S S E .R osendahl,³² P .R osnet,³¹ P .R ukoyatkin,²² V L .R ykov,⁴² B .S ahln ueller,³³ N .Saito,^{27,42,43} T .S akaguchi,³
 S .Sakai,⁵³ H .S akata,¹⁷ V .S am sonov,⁴¹ S .S ato,²³ S .S awada,²³ J .S eele,⁸ R .S eidl,¹⁹ V .S emanov,¹⁸ R .Seto,⁴
 D .Sharma,⁵⁶ I .Shein,¹⁸ A .Shevel,^{41,48} T .A .S hibata,^{42,52} K .Shigaki,¹⁷ M .Shim oura,⁵³ K .Shoji,^{27,42}
 A .Sickles,⁴⁹ C L .Silva,⁴⁶ D .Silvermyr,³⁸ C .Silvestre,¹¹ K .S .Sim,²⁵ C P .S ingh,² V .Singh,² S .Skutnik,²¹
 M .Slunecka,^{5,22} A .S oldatov,¹⁸ R A .S oltz,²⁹ W E .S ondheim,³⁰ S P .S orensen,⁵¹ I V .S ourikova,³ F .Staley,¹¹
 P W .S tankus,³⁸ E .S tenlund,³² M .Stepanov,³⁷ A .S ter,²⁴ S P .S toll,³ T .S ugitate,¹⁷ C .Suire,³⁹ J .Szklai,²⁴
 T .Tabaru,⁴³ S .Takagi,⁵³ E M .T akagui,⁴⁶ A .T aketani,^{42,43} Y .T anaka,³⁵ K .T anida,^{42,43} M .J .T annenbaum,³
 A .Taranenko,⁴⁸ P .T arjan,¹² T L .Thom as,³⁶ M .T ogawa,^{27,42} A .Toia,⁴⁹ J .Tojo,⁴² L .T oma sek,²⁰ H .T oni,⁴²
 R .S .Towell,¹ V -N .Tram,²⁸ I .T serruya,⁵⁶ Y .T suchimoto,¹⁷ C .V ale,²¹ H .V alle,⁵⁴ H W .van H edke,³⁰
 J .Velkovska,⁵⁴ R .Vertesi,¹² A A .V inogradov,²⁶ M .V irius,¹⁰ V .V rba,²⁰ E .V znuzdaev,⁴¹ M .W agner,^{27,42}
 D .W alker,⁴⁹ X R .W ang,³⁷ Y .W atanabe,^{42,43} J .W essels,³³ S N .W hite,³ D .W inter,⁹ C L .W oody,³ M .W ysoki,⁸

W . X ie,⁴³ Y . Yam aguchi,⁵⁵ A . Yanovich,¹⁸ Z . Yasin,⁴ J . Ying,¹⁶ S . Yokkaichi,^{42,43} G R . Young,³⁸ I . Younus,³⁶
I E . Yushm anov,²⁶ W A . Za jc,^{9,y} O . Zaudtke,³³ C . Zhang,³⁸ S . Zhou,⁶ J . Zim anyi,²⁴, and L . Zolin²²
(PHENIX Collaboration)

¹Abilene Christian University, Abilene, TX 79699, U.S.

²D epartm ent of P hysics, Banaras Hindu University, Varanasi 221005, India

³B rookhaven National Laboratory, Upton, NY 11973-5000, U.S.

⁴U niversity of C alifornia - R iverside, R iverside, CA 92521, U.S.

⁵C harles University, O vocny trh 5, Praha 1, 116 36, Prague, C zech Republic

⁶C hina Institute of Atom ic Energy (CIAE), Beijing, People's Republic of China

⁷C enter for N uclear Study, G raduate School of Science, University of Tokyo, 7-3-1 H ongo, B unkyo, Tokyo 113-0033, Japan

⁸U niversity of Colorado, Boulder, CO 80309, U.S.

⁹C olumbia U niversity, New York, NY 10027 and Nevis Laboratories, Irvington, NY 10533, U.S.

¹⁰C zech Technical U niversity, Z ikova 4, 166 36 Prague 6, C zech Republic

¹¹D apnia, CEA Saclay, F-91191, G if-sur-Y vette, France

¹²D ebrecen University, H -4010 D ebrecen, E gyetem ter 1, Hungary

¹³E LTE , E otvos Lorand U niversity, H - 1117 Budapest, P azm any P . s. 1/A , Hungary

¹⁴F lorida Institute of Technology, M elbourne, FL 32901, U.S.

¹⁵F lorida State U niversity, Tallahassee, FL 32306, U.S.

¹⁶G eorgia State U niversity, Atlanta, GA 30303, U.S.

¹⁷H iroshima U niversity, K agam iyama, H igashi-H iroshima 739-8526, Japan

¹⁸IHEP P rotvino, State Research C enter of Russian Federation, Institute for H igh E nergy P hysics, P rotvino, 142281, Russia

¹⁹U niversity of Illinois at Urbana-Champaign, Urbana, IL 61801, U.S.

²⁰Institute of P hysics, A cademy of Sciences of the C zech Republic, Na Slovance 2, 182 21 Prague 8, C zech Republic

²¹Iowa State U niversity, Ames, IA 50011, U.S.

²²J oint Institute for N uclear Research, 141980 D ubna, M oscow Region, Russia

²³K EK , H igh E nergy A ccelerator Research O rganization, T sukuba, Ibaraki 305-0801, Japan

²⁴K FK I Research Institute for P article and N uclear P hysics of the H ungarian A cademy of Sciences (M TA K FK I RM K I), H -1525 Budapest 114, P O Box 49, Budapest, Hungary

²⁵K orea U niversity, Seoul, 136-701, K orea

²⁶R ussian Research C enter "K urchatov Institute", M oscow, Russia

²⁷K yoto U niversity, K yoto 606-8502, Japan

²⁸L aboratoire Leprince-R inguet, E cole Polytechnique, CNRS-IN2P3, Route de Saclay, F-91128, Palaiseau, France

²⁹L awrence Livermore N ational Laboratory, Livermore, CA 94550, U.S.

³⁰L os Alamos N ational Laboratory, Los Alamos, NM 87545, U.S.

³¹L PC , U niversite Blaise P ascal, CNRS-IN2P3, C lemont-F d, 63177 A ubiere Cedex, France

³²D epartm ent of P hysics, Lund U niversity, Box 118, SE-221 00 Lund, Sweden

³³I nstitut f ur K emphysik, U niversity of M uenster, D -48149 M uenster, Germany

³⁴M yongji U niversity, Yongin, Kyonggi-do 449-728, K orea

³⁵N agasaki Institute of Applied Science, N agasaki-shi, N agasaki 851-0193, Japan

³⁶U niversity of New M exico, Albuquerque, NM 87131, U.S.

³⁷N ew M exico State U niversity, Las C ruces, NM 88003, U.S.

³⁸O ak Ridge N ational Laboratory, Oak Ridge, TN 37831, U.S.

³⁹I PN -O rsay, U niversite Paris Sud, CNRS-IN2P3, BP 1, F-91406, O rsay, France

⁴⁰P eking U niversity, Beijing, People's Republic of China

⁴¹P N P I, Petersburg N uclear P hysics Institute, G atchina, Leningrad region, 188300, Russia

⁴²R IKEN , T he Institute of P hysical and C hemical R esearch, W ako, Saitama 351-0198, Japan

⁴³R IKEN BNL Research C enter, Brookhaven N ational Laboratory, Upton, NY 11973-5000, U.S.

⁴⁴P hysics D epartm ent, R ikyo U niversity, 3-34-1 N ishi-Ikebukuro, Toshima, Tokyo 171-8501, Japan

⁴⁵Saint Petersburg State P olytechnic U niversity, St. Petersburg, Russia

⁴⁶U niversidade de S ao P aulo, Instituto de F sica, Caixa Postal 66318, S ao P aulo CEP 05315-970, B razil

⁴⁷S ystem E lectronics Laboratory, Seoul N ational U niversity, Seoul, South K orea

⁴⁸C hem istry D epartm ent, Stony Brook U niversity, Stony Brook, SUNY, NY 11794-3400, U.S.

⁴⁹D epartm ent of P hysics and A stronomy, Stony Brook U niversity, SUNY, Stony Brook, NY 11794, U.S.

⁵⁰S UBATECH (E cole des M ines de N antes, CNRS-IN2P3, U niversite de N antes) BP 20722 - 44307, N antes, France

⁵¹U niversity of Tennessee, K noxville, TN 37996, U.S.

⁵²D epartm ent of P hysics, Tokyo Institute of Technology, O h-okayama, Meguro, Tokyo 152-8551, Japan

⁵³I nstitute of P hysics, U niversity of T sukuba, T sukuba, Ibaraki 305, Japan

⁵⁴Vanderbilt U niversity, N ashville, TN 37235, U.S.

⁵⁵W aseda U niversity, Advanced Research Institute for Science and

Engineering, 17 K ikui-cho, Shinjuku-ku, Tokyo 162-0044, Japan

⁵⁶W eizmann Institute, Rehovot 76100, Israel

⁵⁷Y onsei U niversity, IPAP, Seoul 120-749, K orea

(D ated: April 15, 2024)

$J=$ production in $p+p$ collisions at $\sqrt{s} = 200$ GeV has been measured in the PHENIX experiment at the Relativistic Heavy Ion Collider (RHIC) over a rapidity range of $-2.2 < y < 2.2$ and a transverse momentum range of $0 < p_T < 9$ GeV/c. The statistics available allow a detailed measurement of both the p_T and rapidity distributions and are sufficient to constrain production models. The total cross section times branching ratio determined for $J=$ production is $B_{11}^{J=} = 178^{stat} 53^{sys} 18^{norm}$ nb.

PACS numbers: PACS numbers:

$J=$ are produced in hadronic collisions involving hard processes that proceed primarily through diagrams involving gluons, such as gluon-gluon fusion. Once the cc pair is produced it must evolve through a hadronization process to form a physical $J=$. While this production has been extensively studied, the details of the production mechanism and hadronization remain an open question. Attempts at a consistent theoretical description of $J=$ production have been made, but it has proven difficult to reproduce both the observed cross sections and polarization [1, 2, 3, 4]. An additional complication is that nearly 30-40% of the measured $J=$ yield results from feeddown of higher mass states (', '') [5], reducing the observed polarization with respect to that expected from directly produced $J=$.

The color-singlet model [6], which generates a color singlet cc pair in the same quantum state as the $J=$, underpredicts the measured $J=$ cross section by approximately an order of magnitude [2]. Alternatively, the color-octet model includes color octet cc pairs that radiate soft gluons during $J=$ formation [7]. However, the color octet matrix elements are not universal [8] and the predicted transverse $J=$ polarization at high p_T is not seen in the data [2, 4]. The color evaporation model, a more phenomenological approach, forms the di erent charmonium states in proportions determined from experimental data for any cc pair that has a mass below the D D threshold and predicts no polarization. Finally, a recent perturbative QCD calculation including 3-gluon diagrams is able to successfully reproduce both the observed cross section and polarization results [9].

A fundamental understanding of the $J=$ production process is also critical to defining the con guration of the produced cc state since this will have direct implications on the interaction of this state with both cold nuclear matter in proton or deuteron-nucleus collisions and with the high-density partonic matter observed in high-energy heavy-ion collisions. High quality experimental results over wide kinematical and collision energy ranges are required to constrain models and to provide an improved understanding of $J=$ (and other heavy quarkonia) production.

In this paper, $J=$ production in $p+p$ collisions at $\sqrt{s} = 200$ GeV measured by the PHENIX experiment at RHIC is reported. The $J=$ cross section and transverse momentum distributions are studied in the mid ($|y| < 0.35$) and forward ($1.2 < |y| < 2.2$) rapidity re-

gions. The data presented were collected during the 2005 RHIC run and exceed by more than one order of magnitude the previously reported number of $J=$ [10, 11].

A detailed description of the PHENIX experiment is provided in [12]. At mid-rapidity the drift chambers (DC), ring imaging Cerenkov detectors (RICH), and electromagnetic calorimeters (EMCal) are used to detect $J= + - e^+ e^-$ decays in two arms each covering $= 90^\circ$ in azimuth. The muon detectors, consisting of cathode strip tracking chambers in a magnetic field (MuTr) and alternating layers of steel absorber and Tarcocci tube planes (MuID), are used to measure $J= + +$ at forward and backward rapidities over $= 360^\circ$.

The data were recorded using a minimum bias trigger that requires at least one hit in each of the beam-beam counters (BBC) at forward and backward rapidity, $3.0 < |j| < 3.9$. Dielectron events must pass an additional trigger that consisted of an OR between the level-1 electron and photon triggers. The electron trigger requires matching hits between the EM Cal and RICH in a small angular area with a minimum energy deposition of 0.4 GeV in any 2×2 patch of EM Cal towers. The photon trigger requires a minimum energy deposition of 1.4 GeV in any 4×4 set of overlapping EM Cal towers. A $J=$ trigger efficiency of 96% was achieved within the vertex range $|z_{vtx}| < 30$ cm. Dimuon triggered events were selected using an online level-1 trigger that requires at least two particles penetrate the MuID. One particle must penetrate the entire MuID while the second has a minimum penetration depth of 3 out of the 5 pairs of detector and absorber planes. Approximately 92% of the $J=$'s within $|z_{vtx}| < 30$ cm fulfill this requirement. As part of the reconstruction chain a level-2 filter, which consists of a fast reconstruction of the particle trajectory in the MuTr and MuID is applied. Events are accepted by this filter when at least two particles penetrate the entire MuID and have a reconstructed invariant mass 2.0 GeV/c 2 . After applying cuts on the collision vertex position and quality assurance criteria, the sampled statistics corresponds to 2.6 pb^{-1} in the dielectron analysis, 2.7 pb^{-1} in the muon arm covering $1.2 < |y| < 2.2$ and 3.5 pb^{-1} in the muon arm covering $2.2 < |y| < 1.2$.

At mid-rapidity electron candidates are charged tracks associated with at least two hit phototubes in the RICH and one EM Cal hit with a position matching of 4 standard deviations (). The energy-momentum matching requirement is $(E_{\text{rec}} - E_{\text{true}})^2 / (E_{\text{true}}^2) = -4.0$. The number of $J=$

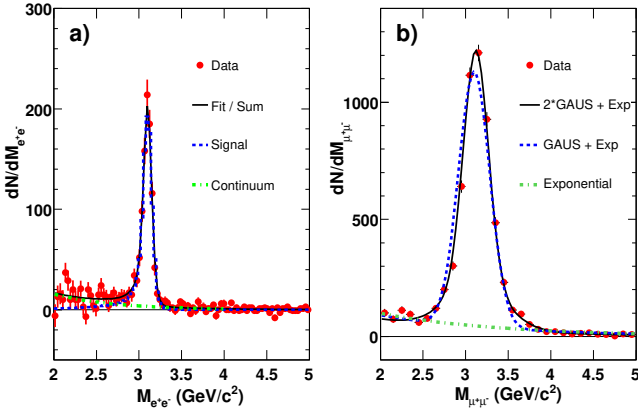


FIG. 1: Invariant mass spectra for a) $J=+1$ e^+e^- at $0.35 < |y| < 0.5$ and b) $J=+1$ $\mu^+\mu^-$ at $1.2 < |y| < 2.2$ with the functional form used to extract the number of reconstructed $J=+1$.

is obtained by counting the un-like-sign dielectron pairs in a fixed mass window after subtracting the like-sign pairs. Figure 1(a) shows the invariant mass spectrum for dielectron pairs after subtracting the like-sign background. The mass window for counting the $J=+1$ signal is $2.7 - 3.5$ GeV/c^2 or $2.6 - 3.6$ GeV/c^2 depending on the number of the DC hits used to reconstruct the track. The $J=+1$ counts are corrected for the continuum yield, which originates primarily from open charm pairs and Drell-Yan, inside the mass window (10% – 5%) and the fraction of $J=+1$ outside of the mass window (7.2% – 1.0%). Approximately 1500 $J=+1$ e^+e^- are obtained. The solid line in the figure is the sum of the $J=+1$ line shape (dashed curve) and an exponential function (dot-dashed curve) describing the continuum component. The $J=+1$ line shape function includes the detector resolution, the internal radiative effect [13], and the external radiative effect evaluated using a GEANT [14] simulation of PHENIX detector.

Meson track candidates are selected based upon their penetration depth in the MuID and the reconstructed track quality within the MuID and MuTr. The particle trajectory must contain at least 8 of 10 possible hits in the MuID and the position matching between the MuID and MuTr must be within 15 (20) cm at positive (negative) rapidity. The $J=+1$ yield is obtained from the un-like sign dimuon invariant mass distribution by subtracting the combinatorial background estimated using an event mixing technique. Three functions, shown in Fig. 1(b), are used to extract the $J=+1$ yield. Single Gaussian + exponential and double Gaussian + exponential functions are used to fit the $J=+1$ peak, while the contribution from the physical continuum and background is estimated using an exponential fit. The reported number of $J=+1$ represents the average of the fit values. A total of 8000 $J=+1$ $\mu^+\mu^-$ are obtained. The systematic error associated with the signal extraction is estimated from the

variation between the fits.

The $J=+1$ cross section in a given rapidity and transverse momentum bin is calculated according to,

$$\frac{B_{11}}{2 \pi r} \frac{d^2 \sigma_{J=+1}}{dy dp_T} = \frac{1}{2 \pi r p_T Y} \frac{N_{J=+1}}{L A_{\text{rec}} \epsilon_{\text{trig}}^{BBC}};$$

where B_{11} is the $J=+1$ dilepton branching ratio, $N_{J=+1}$ is the measured $J=+1$ yield, L is the integrated luminosity recorded by the minimum bias trigger, A_{rec} represents the geometrical acceptance and reconstruction efficiency, and ϵ_{trig} is the trigger efficiency. $\epsilon_{\text{BBC}}^{BBC}$ is the minimum bias trigger efficiency for events containing a $J=+1$ and was determined to be 0.79 ± 0.02 [10]. The cross section sampled by the BBC trigger, $\frac{\text{pp}}{\text{tot}} \epsilon_{\text{BBC}}^{BBC} = 23.0 \pm 2.2 \text{ mb}$, was used to determine the integrated luminosity.

The A_{rec} and ϵ_{trig} terms are determined individually for the central arm and each muon arm based upon the detection of simulated $J=+1$ processed using the real data analysis chain. Decay events are generated and propagated through a full GEANT simulation of the detector, which includes the specific details of the detector performance including the MuTr and MuID alignment, disabled anodes and MuID efficiency. For the dielectron analysis, corrections to account for the detector dead channel map, energy calibration and run-to-run variations in the detector active area were determined from single electron yields. The $J=+1$ trigger efficiency is incorporated via a level-1 trigger emulator tuned to describe the experimental trigger response. For the dimuon analysis, the level-2 filtering algorithms are applied to the simulated events. After reconstruction, the number of detected $J=+1$ is compared to the number of simulated $J=+1$ in a given rapidity and transverse momentum bin to determine the appropriate correction factors.

The systematic error associated with the measurement of the $J=+1$ cross section can be divided into three categories based upon the effect each error has on the measured results. All errors are reported as standard deviations. Point-to-point uncorrelated errors, such as the signal extraction systematic, which is bin dependent with typical values of 4% (5%) in the dimuon (dielectron) data, allow the data points to move independently with respect to one another. Point-to-point correlated errors allow the data points to move coherently within the quoted value. Their values amount to 10% (8%) for the detector acceptance, 8% (4%) for the run-to-run variation in the detector efficiency, 4% (2.5%) for the $J=+1$ transverse momentum and vertex distributions, and 2% (2%) for the hardware efficiency of the detector. Finally, global systematic errors allow the data points to move together. The dominant source of this error originates from the estimation of the BBC triggering efficiency for minimum bias events, 9.7%, with additional contribution from the uncertainty in the estimation of the number of sampled minimum bias events, 1%, and $\epsilon_{\text{BBC}}^{BBC}$, 2.5%.

Figure 2 (a) shows the transverse momentum spectra at both mid and forward rapidities, which are fitted with the function, $A(1 + (p_T/B)^2)^{-6}$ [15], to extract the $\langle p_T^2 \rangle$. At mid-rapidity $\langle p_T^2 \rangle_i = 4.14 \pm 0.18 \pm 0.30$ (GeV/c^2)² and the χ^2/ndf per degree of freedom (χ^2/ndf) is 23=19. At forward rapidity $\langle p_T^2 \rangle_i = 3.59 \pm 0.06 \pm 0.16$ (GeV/c^2)² and the χ^2/ndf is 28=17. The first error is statistical and the second includes the systematic error from the maximum shape deviation permitted by the point-to-point correlated errors and from allowing the exponent of the t function to be a free parameter. Although good agreement is found with the rapidity distribution and total cross section, previously published results [11] yielded a significantly lower $\langle p_T^2 \rangle_i$ at forward rapidity than found here, even accounting for the quoted statistical and systematic uncertainties. The increased statistics of the present data set allow for an improved understanding of the shape of the p_T spectrum at forward rapidity due to the extended range in p_T and the finer binning at low p_T . The previous results have been revisited and it was found that the systematic error was underestimated.

Figure 2 (b) shows the ratio of the invariant cross section at forward and mid-rapidity. The ratio falls with p_T and reaches a minimum of 0.5 above a p_T of 2 GeV/c . The data indicates that the forward rapidity p_T distribution is substantially softer than mid-rapidity. This is attributed to the increase in the longitudinal momentum at forward rapidity leaving less energy available in the transverse direction.

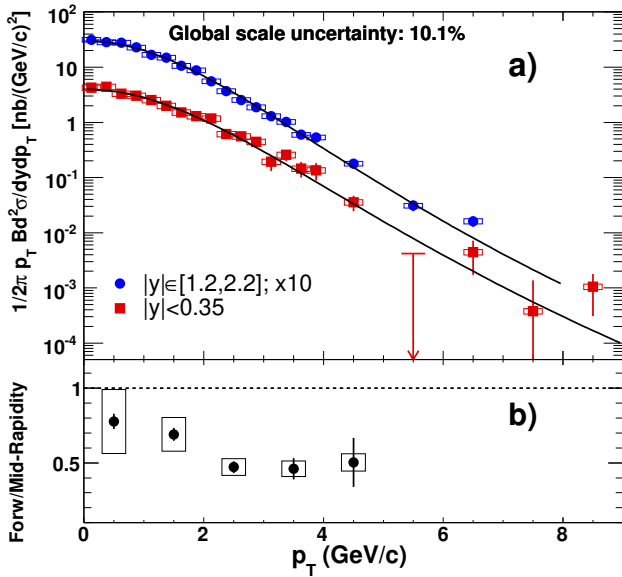


FIG. 2: (a) The mid and forward rapidity J/ψ differential cross section times dilepton branching ratio versus p_T and (b) the ratio of the mid and forward p_T spectra. The vertical error bars are the statistical and point-to-point uncorrelated error and the boxes are the point-to-point correlated systematic error. The solid lines are the fits described in the text.

The observed p_T distributions are substantially harder

than those for lower energy $p+p$ and $p+A$ collisions as expected from the increased phase space at higher energy. Figure 3 shows the energy dependence of the average $\langle p_T^2 \rangle_i$ including lower energy points from the Super Proton Synchrotron, and Fermilab fixed target and Tevatron measurements. A linear fit versus the log of the center-of-mass energy describes the general trends, although some variation is expected due to the differing rapidity ranges of the measurements and the use of $p+A$ data for some of the points.

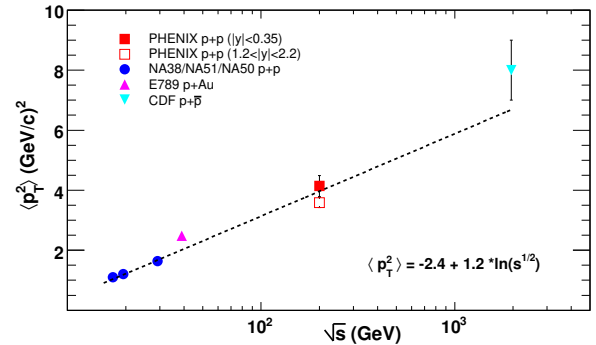


FIG. 3: PHENIX $\langle p_T^2 \rangle_i$ measurements compared to measurements at other energies [4, 16, 17] as a function of collision energy for J/ψ production in $p+p$ or $p+A$ collisions. Also shown is a linear fit vs $\ln(\sqrt{s})$.

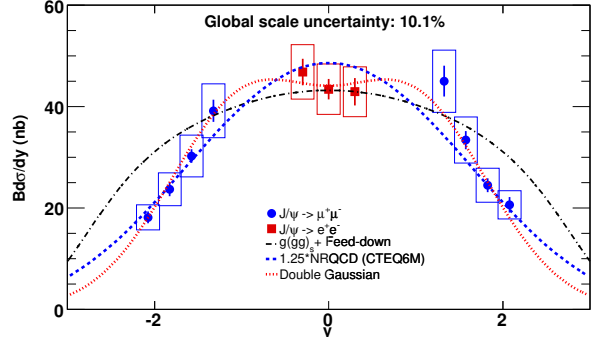


FIG. 4: The J/ψ differential cross section times dilepton branching ratio plotted versus rapidity. The vertical error bars represent the statistical and point-to-point uncorrelated error and the boxes represent the point-to-point correlated systematic error. The curves are described in the text.

Figure 4 shows the J/ψ differential cross section vs rapidity. The statistics of these results are large enough to allow eleven rapidity bins to be measured compared to the five bins used in the previous measurement [11]. Also shown are several models to the data. The dashed curve is a non-relativistic QCD calculation [18]. The dot-dash curve is a pQCD calculation that includes diagrams describing a third gluon, which is necessary to neutralize the otherwise colored states [9]. This model fails to reproduce the steeply falling cross section observed in

the present data at large rapidity. An empirical double Gaussian fit (dot-dot curve) is able to reproduce the data best, but has no strong theoretical foundation. The data slightly favor a flatter distribution over the rapidity range $|y| < 1.5$ than most models, but since the systematic error on the mid and forward rapidity points are independent, a narrower distribution is not excluded.

To determine the total cross section, the rapidity distribution was fitted with many theoretical and phenomenological shapes, including those shown in Fig. 4. We obtain a total cross section times branching ratio of $B_{J/\psi}^{pp} = 178 \pm 3^{stat} \pm 53^{sys} \pm 18^{norm} \text{ nb}$. The absolute normalization error (norm) represents the uncertainty in the BBC trigger cross section. The systematic error (sys) is estimated from the maximum variation allowed by shifting the mid and forward rapidity data independently by their point-to-point correlated systematic errors. This result is consistent with our previous measurement [11].

We have presented J/ψ results for $p_T^{\psi} > 15 \text{ GeV}$ that extend the reach in transverse momentum to $9 \text{ GeV}/c$. The measured p_T^{ψ} spectrum is harder than that observed at lower energies and also shows a softening at forward rapidity. The rapidity shape falls steeply at forward rapidity and can not be reproduced by the pQCD calculation in [9]. Furthermore, the data slightly favor a flatter rapidity distribution than most models, but a narrower distribution is not excluded. These data not only constrain production models for heavy quarkonia, but also provide a critical baseline for similar studies in deuteron-nucleus and heavy-ion collisions [19, 20].

We thank the staff of the Collider-Accelerator and Physics Departments at BNL for their vital contributions. We acknowledge support from the Department of Energy and NSF (USA), MEXT and JSPS (Japan), CNPq and FAPESP (Brazil), NSFC (China), MSM (Czech Republic), IN2P3/CNRS, and CEA (France), BMWF, DAAD, and AvH (Germany), OTKA (Hungary), DAE (India), ISF (Israel), KRF and KOSEF (Korea), MES, RAS, and FFAE (Russia), VR and KAW (Sweden), US-CRDF for the FSU, US-Hungarian NSF-

OTKA-MTA, and US-Israel BSF.

D deceased

- ^y PHENIX Spokesperson: za.j@nevis.columbia.edu
- [1] M. Beneke, M. Kraemer, Phys. Rev. D 55, 5269 (1997); M. Beneke, I.Z. Rothstein, Phys. Rev. D 54, 2005 (1996).
 - [2] F. Abe et al., Phys. Rev. Lett. 69, 3704 (1992); F. Abe et al., Phys. Rev. D 66, 092001 (2002); S. Abachi et al., Phys. Lett. B 370, 239 (1996); B. Abbott et al., Phys. Rev. Lett. 82, 35 (1999).
 - [3] R. Vogt, Phys. Repts. 310, 197 (1999).
 - [4] M. H. Schub et al., Phys. Rev. D 52, 1307 (1995).
 - [5] I. Abt et al., Phys. Lett. B 561, 61 (2003).
 - [6] E.L. Berger et al., Phys. Rev. D 23, 1521 (1981); R. Baier et al., Phys. Lett. B 102, 364 (1981).
 - [7] G.T. Bodwin et al., Phys. Rev. D 51, 1125 (1995); erratum Phys. Rev. D 55, 5853 (1997).
 - [8] J.K. Mizukoshi, SLAC-PUB-8296, hep-ph/9911384 (1999).
 - [9] V.A. Khoze et al., Eur. Phys. J. C 39, 163–171 (2005) and private communications.
 - [10] S.S. Adler et al., Phys. Rev. Lett. 92, 051802 (2004).
 - [11] S.S. Adler et al., Phys. Rev. Lett. 96, 012304 (2006).
 - [12] K. Adcox et al., Nucl. Instr. Meth. A 499, 469 (2003).
 - [13] A. Spiridonov, hep-ex/0510076 (2004).
 - [14] GEANT 3.2.1, CERN Computing Library,
<http://wwwasd.web.cern.ch/wwwasd/geant/index.html>.
 - [15] J.K. Yoh et al., Phys. Rev. Lett. 41, 684 (1978); and private communication..
 - [16] O. Dрапиер, These d'habilitation, Université Claude Bernard – Lyon 1, 1998; available at <http://na50.web.cern.ch/NA50/theses.html>.
 - [17] D.A. Costa et al., Phys. Rev. D 71, 032001 (2005). The $\frac{dp_T^2}{dt}$ was extracted using a fit of the form $A \cdot (1 + (p_T/B)^2)^6$.
 - [18] F. Cooper et al., Phys. Rev. Lett. 93, 171801 (2004); and private communication.
 - [19] S.S. Adler et al., (Au+Au J/ψ paper, preprint number soon).
 - [20] S.S. Adler et al., (Cu+Cu J/ψ paper, preprint number soon).